Wavelength and decay length of density overshoot structure in supercritical, collisionless bow shocks

R. Saxena and S. D. Bale
Department of Physics and Space Sciences Laboratory, University of California, Berkeley, California 94720-7450

T. S. Horbury
The Blackett Laboratory, Imperial College, London, United Kingdom

(Received 25 October 2004; accepted 7 March 2005; published online 9 May 2005)

Above some critical Mach number, quasiperpendicular collisionless shocks are known to exhibit "overshoot" and "undershoot" structure thought to be associated with the motion of ions trapped at the shock front. Using spacecraft potential data from the Cluster spacecraft, the overshoot/undershoot density structure at 56 crossings of the quasiperpendicular bow shock is studied. The envelope of the absolute value of the density, in most cases, decays exponentially and these envelopes are fitted to a decaying function from which we calculate the decay length scale. The overshoot/undershoot wavelength is also estimated using the zero crossings of the density profile and a good correlation between the average wavelength and the convected ion gyroradius is found: the wavelength is approximately two to three times the ion gyroradius. There is no evidence of a strong correlation between the wavelength and the ion inertial length. Similar results are found for the decay length, which also seems to be ordered by the convected ion gyroradius. © *2005 American Institute of Physics*. [DOI: 10.1063/1.1900093]

I. INTRODUCTION

The super-Alfvénic solar wind is shocked and heated upstream of the terrestrial magnetosphere in a standing fast-mode collisionless shock. Although the dissipation mechanism at collisionless shocks is not fully understood, there is an expected transition from resistive/dispersive dissipation at low Mach numbers to a viscous interaction at higher Mach numbers. For a $\beta=0$, perpendicular shock, the transition occurs at a "critical" Mach number $M_c \approx 2.76$.[1,2] Subcritical shocks ($M<M_c$) can balance the nonlinear steepening with wave dispersion[2] and/or some anomalous resistivity;[3] hence subcritical shocks can be modeled using fluid equations with some *ad hoc* resistive term. However, the "viscous" dissipation required at supercritical ($M>M_c$) shocks is thought to be provided by motion of ions trapped, and circulating, in the shock front. There is no simple, analytical term that provides closure to the fluid equations for this kinetic physics.

Ion motion in supercritical, quasiperpendicular shock fronts is complicated. A fraction of the incident ions are (specularly) reflected and gyrate around the shock ramp before cycling downstream, while the majority of the ions are transmitted through the shock and move downstream.[4,5]

Supercritical shocks exhibit a phenomenon known in the literature as "overshoot," in which the magnetic field just downstream of the shock ramp is observed to overshoot (and then undershoot) the asymptotic value;[6] qualitatively, this appears similar to the Gibbs phenomenon observed at the Fourier reconstruction of a square wave. This overshoot structure is thought to be related to the transmission and thermalization of the reflected ion population, which moves ballistically through the shock magnetic and electric fields and is, therefore, highly unstable downstream. Computer simulations show that the reflected ion population undergoes a series of gyrations around the shock front,[7,8] interacting with the electric potential and magnetic structure. The decelerated downstream velocity of the gyrating ion population is small and they are prevented from returning to the shock front by the cross-shock electric field; hence they are observed (in simulation) to pile up downstream, forming the density enhancements of the overshoot cycles. Eventually, the gyrating ions are mixed into the transmitted population. In the simulations, this overshoot/undershoot structure is shown to be ordered by the gyroradius of the reflected ions $v_{sw}/\Omega_{i,2}$ and its extent downstream should be a measure of the "mixing" length scale of this population.

An alternative explanation for the overshoot/undershoot structure is that of a decaying instability due to the anisotropic downstream ion distributions.[9] In this scenario, the perturbed ion distributions are unstable and excite electromagnetic ion cyclotron waves, which then relaxes the anisotropy. This physics also predicts a decaying wave form with a wavelength and damping rate of a few ion gyroradii.[10]

Overshoot/undershoot structure at shocks may also play an important role in the eventual heating and energization of the plasma. Giacalone *et al.*[11] showed with test particle simulations that the overshoot enhances ion reflection/acceleration and allows lower energy particles to participate in reflection. Downstream electron heating may also be affected by overshoot structure; Gedalin and Griv[12] commented on the downstream electron anisotropy induced by magnetic overshoots, as the electrons move adiabatically in these fields.

Studies of the magnetic structure of the bow shock abound;[13–15] however, the low cadence (typically several seconds) of particle counting instruments is insufficient to study

shock substructure which typically transits the spacecraft in a few seconds. Here we use spacecraft floating potential measurements as a proxy for electron density, which has the advantage of having very high time resolution. We examine the overshoot/undershoot structure for 56 shocks and measure the "wavelength" and the exponential decay scale. Our wavelength results are consistent with previous measurements of the magnetic field; the measured decay length shows that the mixing of transmitted ions in the shock occurs rapidly downstream.

II. DATA

Data were used from the four Cluster spacecraft. The Cluster mission was launched in 2000 and flies four identical spacecraft in a controlled tetrahedron configuration. The inclined orbit has apogee near 19 Earth radii R_e; therefore, when apogee is on the dayside (between December and May, approximately) Cluster sees at least two shock crossings per orbit. We used data from the first dayside season (2000-2001) when the spacecraft were separated by 500–1000 km.

As discussed above, traditional particle (electron and ion) counting instruments on a spinning spacecraft are often designed to scan in latitude and use the spacecraft spin to sweep the instrument aperture in longitude. This limits the collection time for a three-dimensional distribution function (and therefore moments of the distribution) to 1 spacecraft spin period, which is typically 3–10 s.

The Cluster Electric Field and Waves experiment measures the probe-to-spacecraft and probe-to-probe electric potential using four biased electrostatic probes, deployed orthogonally in the spacecraft spin plane on 44 m wires.[16] For this study, we used spacecraft floating potential data as a proxy for thermal electron density. A sunlit spacecraft emits photoelectrons with a typical *e*-folding energy of 1 eV. In a low density plasma, this causes the spacecraft to charge positive and attract a return current from the local thermal electron population. Strictly speaking, then, the spacecraft potential ϕ_{sc} is a function of the thermal electron current $j_e = n_e e v_{\mathrm{th}} \propto n_e T_e^{1/2}$, where v_{th} is the electron thermal speed and n_e is the electron density. However, geometric effects of the instrument configuration make the dependence on temperature weaker than $T_e^{1/2}$ (Ref. 17) and a good fit between ϕ_{sc} and n_e can usually be found. Here we use a function $n[\phi_{\mathrm{sc}}(t)]$ which is a sum of exponentials where the coefficients were determined by fitting to several hours of ion density data as measured by the electrostatic analysis instrument CIS on Cluster;[18] we compute ϕ_{sc} on each spacecraft as the average of the measured spacecraft potential on the four separate double probes. Spacecraft potential is sampled at 5 samples/s, which allows for sampling of the density structure at the bow shock with multiple data points within the shock structure itself. This data set and calibration were used in Ref. 19 to compute the shock transition scale. Hereafter, we refer to this derived density data as the "density proxy."

Upstream, averaged magnetic field vectors were sampled by the FluxGate Magnetometer instrument on Cluster[20] and used to compute Mach numbers and the shock tangent angle Θ_{bn} (described below). We also use solar wind velocity, temperatures, and He++/H ratio measured by experiments on the ACE spacecraft. These data are convected downstream by the solar wind travel time to correspond temporally to the Cluster shock crossing events.

III. ANALYSIS

We began our analysis by examining 101 quasiperpendicular bow shock crossings from a list of events studied by Bale *et al.*[19] Of this set of shocks, 56 had showed distinct overshoot/undershoot structure in the density proxy data. A few shocks with suspiciously large Mach numbers were excluded from the analysis.

A four-spacecraft timing analysis of the density proxy data was then used to compute the shock normal vector $\hat{n}$ and the speed along the normal v_{sh}.[19] This analysis assumes that the shock is locally planar and not accelerating; shocks that show significantly different temporal profiles between the four-spacecraft were rejected. A calculation of the shock tangent angle Θ_{bn} between the normal vector and average upstream magnetic field showed that all of our shocks are quasiperpendicular ($\Theta_{bn} \geqslant 45°$).

At each shock, a density proxy profile was measured on each of the four-spacecraft and a time lag between spacecraft pairs is computed (as a product of the above timing analysis). All profiles were shifted in time to match, spatially, with the profile of spacecraft 3. We then average the four profiles to obtain an average density profile. The speed of the shock in the spacecraft frame v_{sh}, computed in the timing analysis, is then used to make our temporal measurement a spatial one: $x(t) = v_{\mathrm{sh}} t$.

Figure 1 shows an example of a supercritical, quasiperpendicular shock as used in this analysis; this shock, on December 25, 2000, is magnetosonic Mach number $M_{ms} \approx 4.2$ and $\Theta_{bn} \approx 80°$. To make the overshoot/undershoot structure more easily visible, we fitted the average density profile of each shock to a hyperbolic tangent function, $n(x) = n_0 + n_1 \tanh(x/X)$ and subtract the hyperbolic tangent to leave the remaining "chirp" of the overshoot/undershoot. Panel (b) of Fig. 1 shows the overshoot/undershoot density structure. The hyperbolic tangent function represents an idealized current sheet density profile with no overshoot/undershoot structure and was found to fit well by Bale *et al.*[19] Zero-crossing points of the new profile were selected by hand and the average wavelength λ of the profile was defined as twice the average of the distance between the zeroes [red dots in panel (b)].

To estimate the decay length scale of the overshoot, we computed the absolute value of the average density profile, with the selected zeroes superimposed on top, and selected a peak in the profile between each pair of zeroes [blue triangles in panel (c) of Fig. 1]. An exponential curve $e^{-\beta x}$ (green dotted line) was then fitted to the peaks, from which the decay length was calculated as $\chi_d = 1/\beta$. For those shocks without sufficient data points (three or more) necessary to do an exponential fit, we defined the decay length to be the distance it takes for the density to fall to $1/e$ of the y intercept on our plots, where the $x = 0$ value is arbitrary. The above analysis was applied to the 56 shocks exhibiting

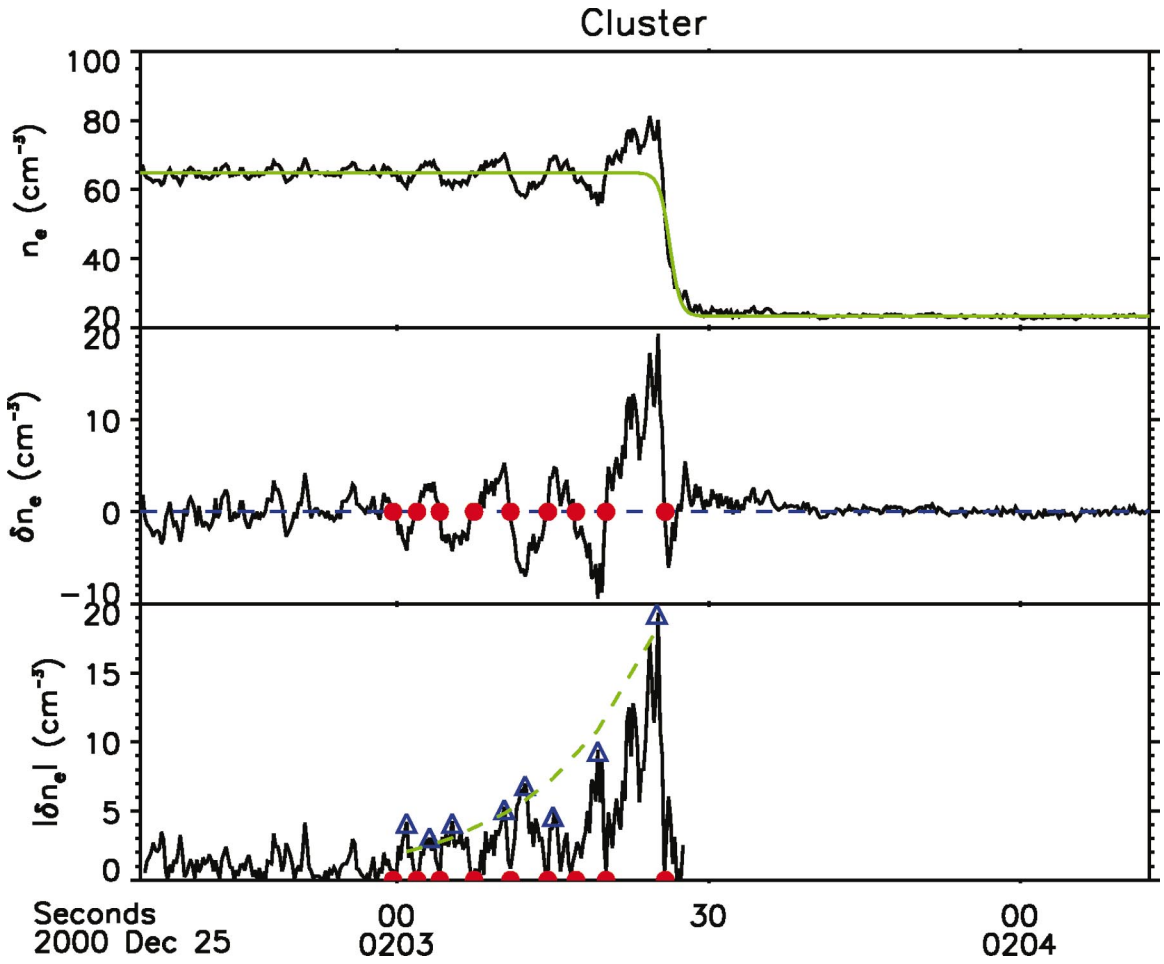

FIG. 1. (Color). Density profiles at a supercritical fast-mode shock. The top panel shows the compressive signature of a fast-mode shock with overshoot/undershoot density structure (black trace) with a hyperbolic tangent fit (green trace). In the middle panel, the hyperbolic tangent has been subtracted leaving the "chirp" signature of the overshoot. Red dots show zero crossings which are used to compute the overshoot/undershoot wavelength. The low panel shows the absolute value of the chirp with blue triangles indicating the maxima between zero crossings. These maxima are fitted with an exponential $e^{-\beta x}$ to obtain a decay length $1/\beta$.

overshoot/undershoot structure. The resulting overshoot wavelengths λ and decay lengths χ_d were then compared to both the upstream ion inertial scale c/ω_{pi}, where ω_{pi} is the ion plasma frequency computed using the upstream ambient density, and the convected ion gyroradius $v_s/\Omega_{ci,2}$. The convected ion gyroradius is computed from v_s, the shock speed in the plasma frame, and $\Omega_{ci,2}$, the ion gyrofrequency downstream of the shock. The convected ion gyroradius is the radius of ions gyrating in the shock front and has previously been shown to be a good measure of overshoot wavelength using magnetic field data[14] and has also been shown to be a good measure of the large scale density transition at the shock.[19]

Histograms of the overshoot wavelength normalized by the ion inertial length $\lambda/(c/\omega_{pi})$ and convected ion gyroradius $\lambda/(v_s/\Omega_{ci,2})$ are shown in Fig. 2 and 3, respectively, in bins of 1. The ion inertial normalization (Fig. 2) gives a rather broad distribution with measures from $\lambda \approx 1$–$16\, c/\omega_{pi}$, while the ion gyro normalization (Fig. 3) is peaked at $\lambda \approx 2$–$3\, v_s/\Omega_{ci,2}$. We take this as evidence that the convected ion gyroradius is the more appropriate normalization. This point will be strengthened below.

A good measure of wavelength and/or decay length might be expected to be consistent over a range of Mach numbers. To test this, we plot our normalized length scales against the magnetosonic Mach number $M_{ms}=v_s/c_{ms}$, where v_s is the shock speed in the plasma frame and $c_{ms}=(v_A^2$

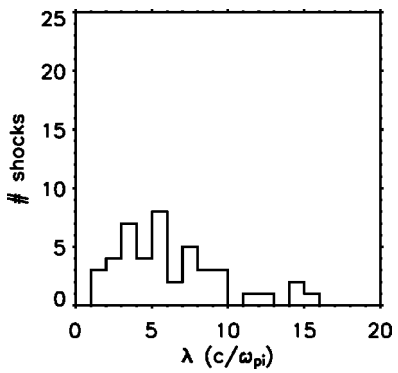

FIG. 2. Histogram of the overshoot/undershoot wavelength normalized to the upstream ion inertial length c/ω_{pi}. This normalization gives a broad distribution in wavelength.

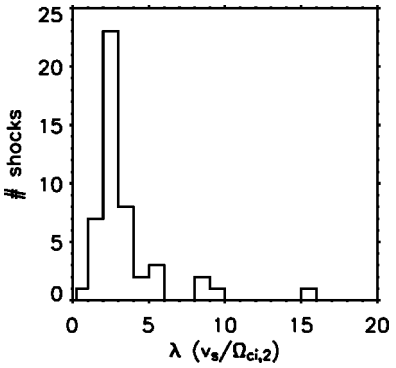

FIG. 3. Histogram of the overshoot/undershoot wavelength normalized to the convected ion gyroradius $v_{sh}/\Omega_{ci,2}$. This normalization gives a more peaked distribution with a maximum between $\lambda \approx (2–3)v_{sh}/\Omega_{ci,2}$; we suggest that this is the appropriate normalization of overshoot/undershoot wavelength.

$+c_s^2)^{1/2}$ is the magnetosonic wave speed (v_A and c_s are the Alfvén and ion sound speeds, respectively). This technique was used by Bale *et al.*[19] to show that the convected ion gyroradius is the measure of the density transition scale.

Figure 4 shows the measured overshoot/undershoot wavelength normalized to the convected ion gyroradius and plotted against Mach number M_{ms}. The error bars are one standard deviation of the points averaged; points with *no* error bar have only point in the bin. While there is scatter in the plot, the values cluster around two to three, as in the histogram of Fig. 3. In Fig. 5, the wavelength is normalized to the ion inertial length and plotted against M_{ms}. In this case, it can be seen that the ratio $\lambda/(c/\omega_{pi})$ increases with Mach number, especially at larger values $M_{ms} \geqslant 5$. Since $(v_s/\Omega_{ci,2})/(c/\omega_{pi}) \propto M$, we see that $\lambda/(c/\omega_{pi}) \propto M\lambda/(v_s/\Omega_{ci,2})$, so that if the convected ion gyroradius is the better measure of overshoot wavelength then $\lambda/(c/\omega_{pi})$ should increase with Mach number, which it does. We can take this as evidence that the gyroradius is the proper measure of density overshoot wavelength. This agrees with the analysis of magnetic field data by Livesey *et al.*[14]

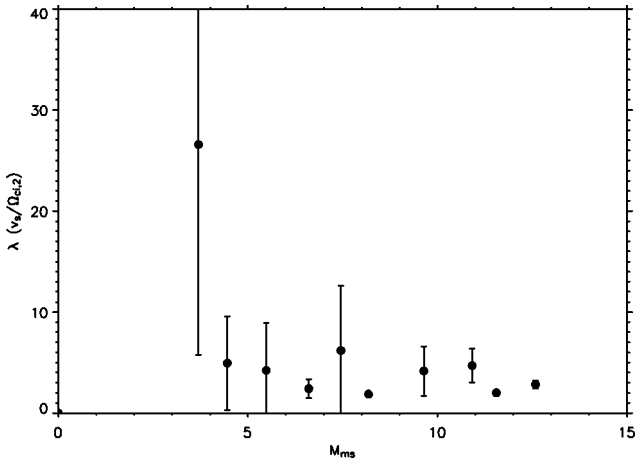

FIG. 4. Overshoot/undershoot wavelength λ normalized to the convected ion gyroscale $v_{sh}/\Omega_{ci,2}$ and plotted against the shock magnetosonic Mach number M_{ms}.

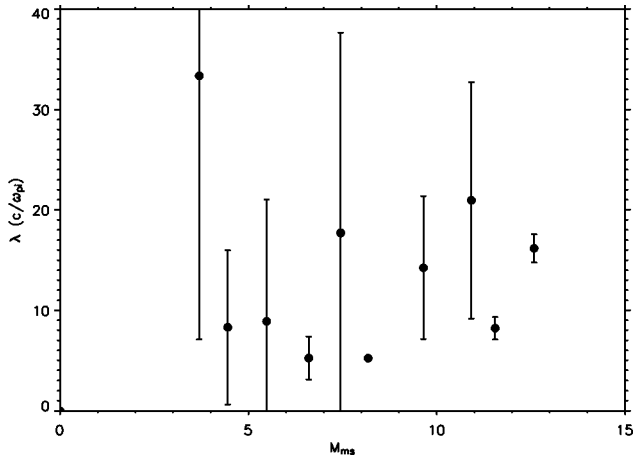

FIG. 5. Overshoot/undershoot wavelength λ normalized to the ion inertial length c/ω_{pi} and plotted against the shock magnetosonic Mach number M_{ms}. An increasing trend is due to the fact that $v_{sh}/\Omega_{ci,2} \propto Mc/\omega_{pi}$, indicating again that the convected ion gyroradius is a better measure of wavelength.

Histograms of the overshoot decay length scale χ_d normalized by the ion inertial length $\chi_d/(c/\omega_{pi})$ and convected ion gyroradius $\chi_d/(v_s/\Omega_{ci,2})$ are shown in Figs. 6 and 7, similar to Figs. 2 and 3. Again, the ion inertial normalization (Fig. 6) gives a rather broad distribution with measures from $\chi_d \approx (1–15)c/\omega_{pi}$, while the ion gyronormalization (Fig. 7) is

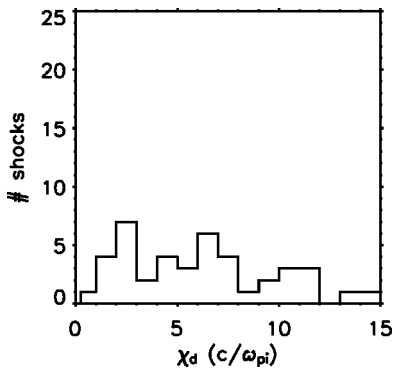

FIG. 6. Histogram of the overshoot/undershoot decay length normalized to the upstream ion inertial length c/ω_{pi}. This normalization gives a broad distribution.

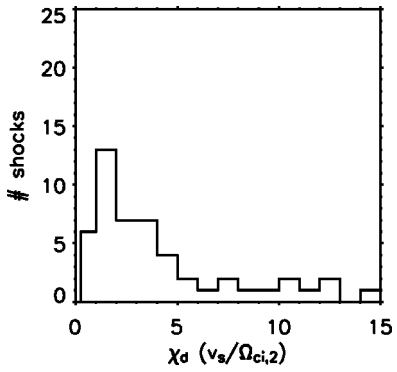

FIG. 7. Histogram of the overshoot/undershoot decay length normalized to the convected ion gyroradius $v_{sh}/\Omega_{ci,2}$. This normalization gives a more peaked distribution with a maximum between $\lambda \approx (1–2)v_{sh}/\Omega_{ci,2}$; we suggest that this is the appropriate normalization of overshoot/undershoot decay scale.

more peaked and takes a most probable value at $\chi_d \approx (1–2) v_s/\Omega_{ci,2}$. We again take this as evidence that the convected ion gyroradius is the more appropriate normalization.

A similar analysis of the decay scale $\chi_d = 1/\beta$ is shown in Fig. 8 and 9. The trend of $\chi_d/(v_s/\Omega_{ci,2})$ with Mach number is again fairly flat, while the ion inertial normalization has much more scatter than for the wavelength (Fig. 5). Still, the ion inertial normalization shows a general increasing trend with Mach number and the above argument can be applied again. Taken together, Fig. 6 and 7 indicate that the appropriate scaling of the exponential decay length of the density overshoot/undershoot is again the convected ion gyroradius. The histogram of $\chi_d/(v_s/\Omega_{ci,2})$ (Fig. 7) gives a most probable value of $\chi_d \approx 1–2 v_s/\Omega_{ci,2}$. The "damping ratio" of a damped simple harmonic oscillator is ratio of the damping coefficient to the value of "critical damping" and is given by $DR = 1/\sqrt{1+(\omega_1/\beta)^2}$, where ω_1 is the observed oscillation frequency. If we consider our overshoot/undershoot to be a damped oscillator, our most probable values of wavelength $(2.5 v_s/\Omega_{ci,2})$ and damping rate $(1.5 v_s/\Omega_{ci,2})$ give a damping ratio of $DR \approx 51\%$, which corresponds to a rather highly damped oscillator.

IV. CONCLUSIONS

An analysis of 56 shocks with overshoot/undershoot structures in the density profiles shows that the average wavelength λ of the profile goes like ~2–3 times the convected ion gyroradius. We concluded that there is no clear correlation between λ and the ion inertial length c/ω_{pi}, except that related back to the convected ion gyroradius; this is consistent with earlier results on magnetic overshoot structure.[14] Additionally, we found that the decay length χ_d of the profile goes like ~1–2 times $v_s/\Omega_{ci,2}$, and again we concluded that there is no clear correlation between χ_d and c/ω_{pi}. Our results show that the overshoot structure is "damped" quickly behind the shock; this implies rapid mixing of the perturbed ion distributions downstream.

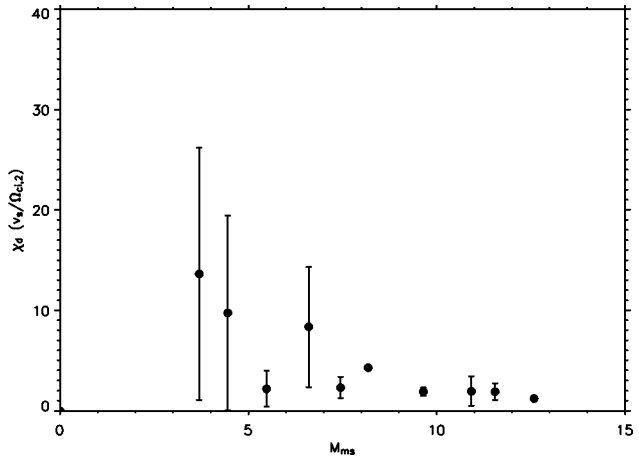

FIG. 8. Overshoot/undershoot decay length χ_d normalized to the convected ion gyroscale $v_{sh}/\Omega_{ci,2}$ and plotted against the shock magnetosonic Mach number M_{ms}. While there is scatter at low Mach number (from four to six), this normalization appears more robust than the ion inertial length.

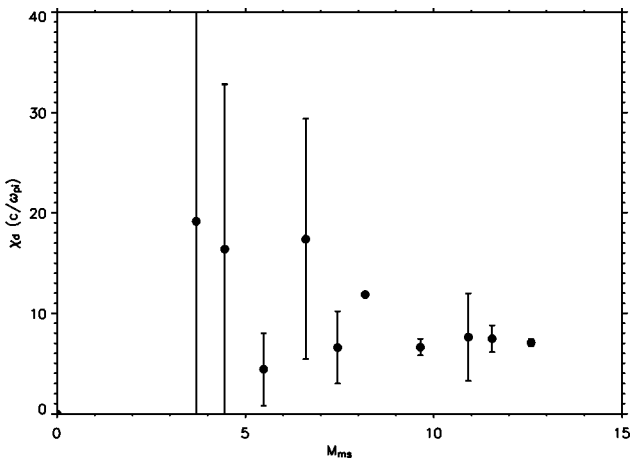

FIG. 9. Overshoot/undershoot decay length χ_d normalized to the upstream ion inertial length c/ω_{pi} and plotted against the shock magnetosonic Mach number M_{ms}. There is considerable scatter perhaps with an increasing trend.

Our measurements of the wavelength of the plasma density profile corroborate results found previously by Livesey *et al.*[14] and in simulations.[7,8] Livesey *et al.*[14] used International Sun-Earth Explorer magnetic field data to show that the thickness of the overshoot (which corresponds to half of our defined wavelength) scales with the ion Larmor radius and is "not nearly so well organized by the ion inertial length." Specifically, they found that the thicknesses of most of their overshoots were one to three times the ion gyroradius; this corresponds to the wavelength being two to six times the ion gyroradius. These numbers are slightly larger than, but consistent with, our results. Qualitatively, the similarity of the density and magnetic field profiles suggests that the overshoot is a magnetohydrodynamics fast-mode phenomenon, like the shock itself; a detailed study of density and field data would be interesting.

ACKNOWLEDGMENTS

Cluster data analysis at University of California, Berkeley was supported by NASA Grant No. NAG5-12483NAG5-11944. T.S.H. was supported by a PPARC(UK) fellowship.

[1] J. P. Edmiston and C. F. Kennel, J. Plasma Phys. **32**, 429 (1984).
[2] C. F. Kennel, J. P. Edmiston, and T. Hada, AGU Monograph Ser. **34**, 1 (1985).
[3] K. Papadopoulos, AGU Monograph Ser. **34**, 59 (1985).
[4] N. Sckopke, G. Paschmann, S. J. Bame *et al.*, J. Geophys. Res. **88**, 6121 (1983).
[5] N. Sckopke, Adv. Space Res. **15**, 261 (1995).
[6] V. G. Eselevich, Planet. Space Sci. **32**, 439 (1984).
[7] M. M. Leroy, C. C. Goodrich, D. Winske *et al.*, Geophys. Res. Lett. **8**, 1269 (1981).
[8] M. M. Leroy, D. Winske, C. C. Goodrich *et al.*, J. Geophys. Res. **87**, 5081 (1982).
[9] M. Tanaka, C. C. Goodrich, D. Winske, and K. Papadopoulos, J. Geophys. Res. **88**, 3046 (1983).
[10] C. S. Wu, D. Winske, M. Tanaka *et al.*, Space Sci. Rev. **37**, 63 (1984).
[11] J. Giacalone, T. P. Armstrong, and R. B. Decker, J. Geophys. Res. **96**, 3621 (1991).
[12] M. Gedalin and E. Griv, J. Geophys. Res. **104**, 14821 (1999).
[13] C. T. Russell, M. M. Hoppe, and W. A. Livesey, Nature (London) **296**, 45 (1982).
[14] W. A. Livesey, C. F. Kennel, and C. T. Russell, Geophys. Res. Lett. **9**, 1037 (1982).

[15]M. M. Mellott and W. A. Livesey, J. Geophys. Res. **92**, 13661 (1987).
[16]G. Gustafsson, R. Bostrom, B. Holback *et al.*, Space Sci. Rev. **79**, 137 (1997).
[17]A. Pedersen, Ann. Geophys. **13**, 118 (1995).
[18]H. Reme, J.-M. Bosqued, J.-A. Sauvaud *et al.*, Space Sci. Rev. **79**, 303 (1997).
[19]S. D. Bale, F. S. Mozer, and T. S. Horbury, Phys. Rev. Lett. **91**, 265004 (2003).
[20]A. Balogh, M. W. Dunlop, S. W. H. Cowley *et al.*, Space Sci. Rev. **79**, 65 (1997).